An Alternative Approach to Assess Water Cycle Intensification at the Global Scale

Mijael Rodrigo Vargas Godoy[1]and Yannis Markonis[1]

[1]Faculty of Environmental Sciences, Czech University of Life Sciences Prague, Kamýcká 129, Praha – Suchdol, 165 00, Czech Republic

Key Points:

- A robust metric for the assessment of water cycle intensification at the global scale is still missing.
- The sum of precipitation and evaporation can improve the detection of the intensification signal.
- The same metric was used to identify potential discrepancies between four reanalysis data sets.

Corresponding author: Mijael R. Vargas Godoy, `vargas_godoy@fzp.czu.cz`

Abstract

The difference between precipitation and evaporation has been extensively used as a metric in various studies to quantify the water budget and to characterize the water cycle's response to global warming. However, when it comes to the global scale, there might be a gap in the information provided by this metric. Herein, we discuss how the sum of precipitation and evaporation could be a complementary alternative to assess global water cycle intensification. To support our argument, we present a brief yet strong correlation and trend analysis of both metrics in four different reanalysis data sets. Our assessment uncovers how a relationship linking atmospheric water fluxes and temperature at the global scale is more comprehensively described by the sum of precipitation and evaporation rather than their difference. Therefore, encouraging the scientific community to include precipitation plus evaporation analyses into their research.

Plain Language Summary

During the past 20 years, researchers across the globe have employed precipitation minus evaporation as a metric to describe the water cycle at multiple scales in time and space. Estimating precipitation minus evaporation helps to evaluate different aspects of the water cycle like the changes due to global warming. At the global scale, however, the information we gain from this metric becomes limited. In this work, we propose the sum of precipitation and evaporation as a complementary alternative. Our assessment revealed that the sum of precipitation and evaporation comprehensively describes the relationship between water cycle intensification and the temperature. As a result future studies can take advantage of the additional information provided by this metric.

1 Introduction

Understanding the global water cycle and its balance is crucial for earth system science and climate change studies. To assess the water cycle at multiple spatiotemporal scales, we observe and measure the fluxes and storage that comprise its budget. Overland, the net water flux into the surface, a vital aspect of the water cycle for human society, is described by the difference between precipitation and evaporation ($P-E$). Thus, $P-E$ characterizes atmosphere-land surface interactions and represents the maximum available renewable freshwater (Oki & Kanae, 2006). Therefore, it is not uncommon to study the behavior of this compound variable rather than solely precipitation or evaporation. Analogously, evaporation minus precipitation ($E - P$) determines the surface salinity of the ocean, which helps determine the stability of the water column (Yu et al., 2020). These two formulations, i.e., $P-E$ and $E-P$, are the most used metrics to assess the current and future intensification of the global water cycle (Allan et al., 2020).

Knowing how much water is available is not enough; we also need to know how it is distributed. Consequently, it is no surprise that there have been numerous efforts to accurately describe the spatiotemporal patterns of $P-E$. There is a consensus that as precipitation increases over land, so does the evaporation over the oceans to balance the global water cycle (Held & Soden, 2006). As a result, standardized $P-E$ over land and the oceans generally mirror each other, suggesting that the precipitation and evapotranspiration offset over land is balanced by the evaporation and precipitation offset over the oceans. Notwithstanding, it has become increasingly evident that there are contrasting responses between the terrestrial and oceanic water cycles (Fasullo, 2010). Zooming out into the global scale and regarding the interannual and longer temporal scales, mean precipitation and evaporation are roughly on par (Pendergrass & Hartmann, 2014), making $P-E$ close to or equal to zero, which unavoidably adds little to no value when evaluating long-term changes in the global water cycle. Hence, the insight gained from $P-E$ on water cycle research appears to be limited by the scale at which it is assessed.

A plausible alternative worth exploring is to use $P+E$ as a complementary metric to assess water cycle variations. At the regional scale, for example, moisture convergence can increase precipitation (Espinoza et al., 2018). Assuming radiation is not limiting, evapotranspiration will be equally enhanced. On the one hand, $P-E$ would suggest no change in the hydrological cycle, while, on the other hand, the increase in $P+E$ would correctly indicate that the water cycle is indeed changing, with more water being circulated in total through the surface-atmosphere continuum. Huntington et al. (2018) have already shown that the sum of precipitation and actual evapotranspiration ($P+$ AET) can be adequately applied to quantify the changes of the terrestrial portion of the water cycle. We argue that this approach can be extended to the description of the whole water cycle because $P+E$ has a robust physical meaning; it describes the total flux of water exchanged between the atmosphere and the surface. Furthermore, just like the human heart, the Earth cycles far more water through the atmosphere than its holding capacity. In this manner, it would make more sense to look into the addition of fluxes rather than their difference when assessing the intensification of the global water cycle.

In this study, we assess four reanalysis data sets using both $P + E$ and $P - E$. First, to explore how $P + E$ holds the potential to complement global water cycle research. Second, to describe some gaps in the information provided by the widely-used metric, $P - E$, at the global scale. Additionally, we discuss the possible connotations of the findings regarding $P+E$ and its application as a performance metric for model simulations and reanalysis data. Our analysis suggests a strong prospect in using the sum of precipitation and evaporation to assess the intensification of the global water cycle.

2 Data and Methods

We selected four reanalysis data products based on the availability of both precipitation and evaporation for a given data set (Table 1). These are the Twentieth Century Reanalysis (20CR) v3 (Slivinski et al., 2019), European Centre for Medium-Range Weather Forecasts (ECMWF) Reanalyses ERA-20C (Poli et al., 2016) and ERA5 (Hersbach et al., 2020), and the National Centers for Environmental Prediction & the National Center for Atmospheric Research NCEP/NCAR Reanalysis 1 (Kalnay et al., 1996). The 20CR v3 estimates assimilate only surface observations of synoptic pressure into NOAA's Global Forecast System throughout the 19th and 20th centuries. ERA-20C is ECMWF's first atmospheric reanalysis of the 20th century, reaching 2010. It assimilates observations of surface pressure and surface marine winds only. ERA5 has replaced the ERA-Interim reanalysis, which stopped on 31 August 2019, and covers 1950-present. It combines vast amounts of historical observations into global estimates using advanced modeling and data assimilation systems. The NCEP/NCAR R1 project uses a state-of-the-art analysis/forecast system to perform data assimilation using past data from 1948 to the present. All of the above data sets are available for download at KNMI Climate Explorer (`https://climexp.knmi.nl/`), as well as on the dedicated websites of their providers.

Table 1. Data Set Overview as Available at KNMI Climate Explorer

Data Set	Spatial Resolution	Record Length	Reference
20CR v3	1°x1°	1836 - 2015	Slivinski et al. (2019)
ERA-20C	~125km	1900 - 2010	Poli et al. (2016)
ERA5	0.25°x0.25°	1979 - now	Hersbach et al. (2020)
NCEP/NCAR R1	T62 gaussian grid[a]	1948 - now	Kalnay et al. (1996)

[a]The T62 gaussian grid has 192 longitude equally spaced and 94 latitude unequally spaced grid points.

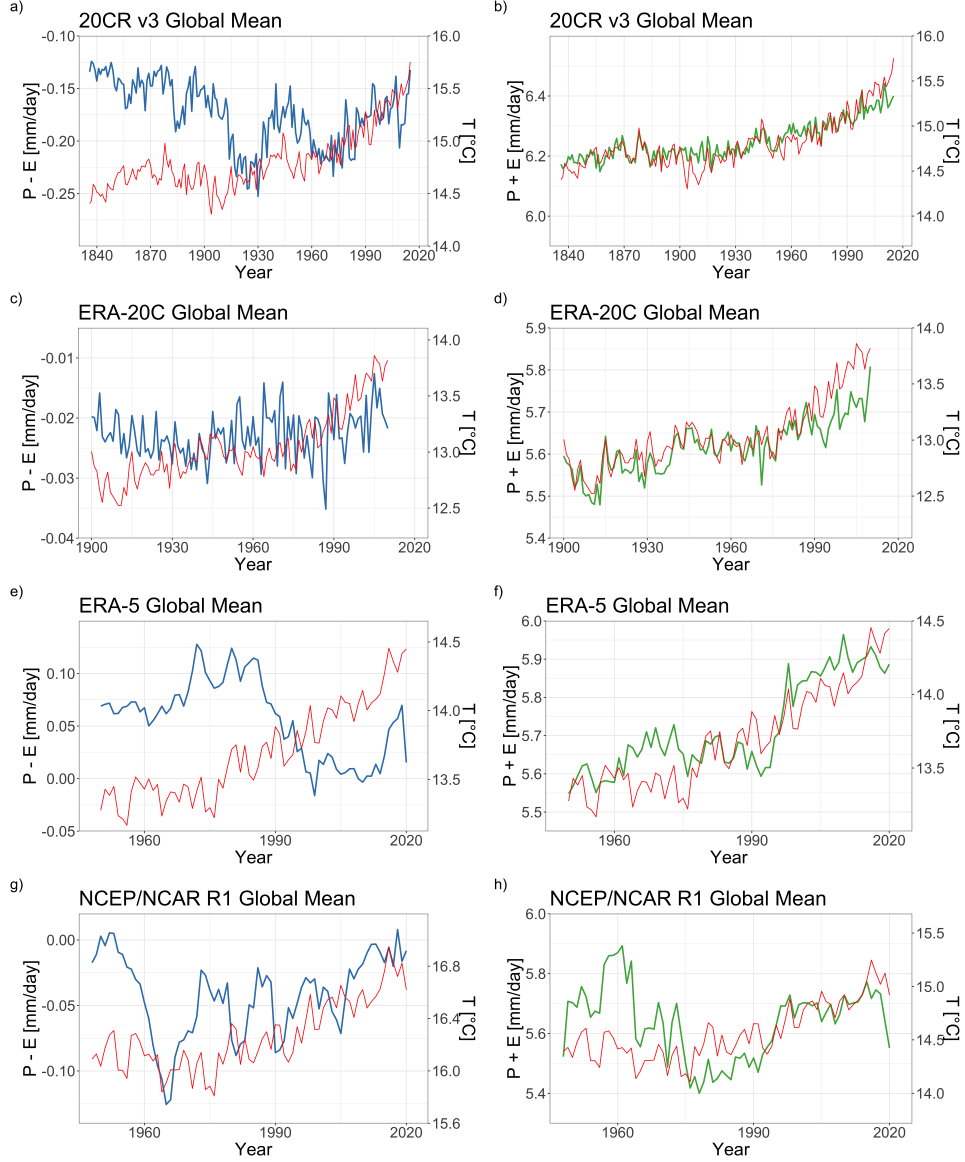We examined different statistical metrics commonly used on time series analyses to compare the traditional approach ($P-E$) and the alternative suggested herein ($P+E$). Through the KNMI Climate Explorer we generated annual mean values for atmospheric water fluxes and global temperature. The linear relationship between atmospheric water fluxes and the temperature was determined via the Pearson correlation coefficient and its statistical significance via the p-value. The same metrics were computed again for the annual differences of each time series. To this extent, we can characterize both the long-term and the year-to-year association between atmospheric water fluxes and temperature. While the correlation coefficient describes the presence or absence of a linear relationship, it does not quantify the rate of change of one variable relative to the other. Henceforth, we used linear regression to estimate the corresponding slopes and describe the rate of change at which atmospheric water fluxes respond to changes in temperature. To compare the slopes between data sets on a one-to-one basis, we estimated atmospheric water fluxes and temperature in terms of global mean anomalies with respect to the 1981-2010 period. To assess the goodness-of-fit of the slopes, i.e., how well these slopes represent the linear relationship between our variables, we relied on the residual standard error.

3 Results

The strength of the $P+E$ metric becomes readily visible by the superimposition of the of the annual mean global temperature and the annual mean global $P+E$ of the four reanalysis data sets (Figure 1). This is further verified by estimating the correlation coefficients of the annual mean global temperature and the annual mean global $P+E$ and $P-E$. The 20CR v3 has the highest correlation of 0.92 with statistical significance p $= 1 \times 10^{-72}$ (Figure 1.b). There is very strong coupling of the two time series, especially up to 1900, while after 1990 the temperature appears to raise more abruptly than the sum of precipitation and evaporation. On the other hand, if we look at $P-E$, we can see no correlation (R = -0.11, p = 0.14; Figure 1.a). The ERA-20C has the second highest correlation for $P + E$ (R = 0.9, p = 5×10^{-41}; Figure 1.d). Once again, we observe a strong coupling of both time series up to 1990, after which the temperature raises more abruptly. Looking into $P-E$, while the correlation is statistically significant, there is a weak association at best (R = 0.25, p = 0.01; Figure 1.c). $P + E$ in ERA-5 has a strong correlation (R = 0.87, p = 2×10^{-22}; Figure 1.f) but unlike the previous two data sets, there is no abrupt temperature raises after 1990. In addition, we can now see that $P - E$ has a moderate negative relationship with temperature (R = -0.6, p = 2×10^{-8}; Figure 1.e). In the case of NCEP/NCAR R1 both $P + E$ (R = 0.35, p = 0.02; Figure 1.h) and $P - E$ (R = 0.41, p = 3×10^{-4}; Figure 1.g) have a moderate positive correlation. Not resembling the other three data sets, NCEP/NCAR R1 has a higher correlation value for the difference than the sum of precipitation and evaporation. Moreover, the strong coupling of $P+E$ and temperature takes place only after 1990.

The superiority of $P+E$ over $P-E$ as a metric to substantiate the relationship between atmospheric water fluxes and temperature carries from the long-term onto the year-to-year. Estimating the annual differences, we observe a general reduction from strong to moderate correlation for $\delta(P+E)$: ERA-20C, which had a correlation of R = 0.9, now has the highest correlation (R = 0.66, p = 7×10^{-15}). ERA-5, which had a correlation of R = 0.87, now has the the second highest correlation (R = 0.63, p = 5×10^{-9}); 20CR v3 has the biggest reduction in correlation from R = 0.92 to R = 0.54 with p = 1×10^{-14}. NCEP/NCAR R1, which had the weakest correlation (R = 0.35), sees an increase in its correlation (R = 0.53, p = 1×10^{-6}). For $\delta(P - E)$, we observe that while some data sets originally had a weak (20CR v3 and ERA-20C) or moderate (ERA-5 and NCEP/NCAR R1) correlation, after estimating annual differences there is no significant correlation present in any data set: ERA-20C (R = 0.128, p = 0.183); ERA-

Figure 1. Average global atmospheric water fluxes in $[mm/day]$ and temperature in $[^\circ C]$, where P is precipitation, E is evaporation, and T is temperature. $P + E$ in green, $P - E$ in blue, and temperature in red.

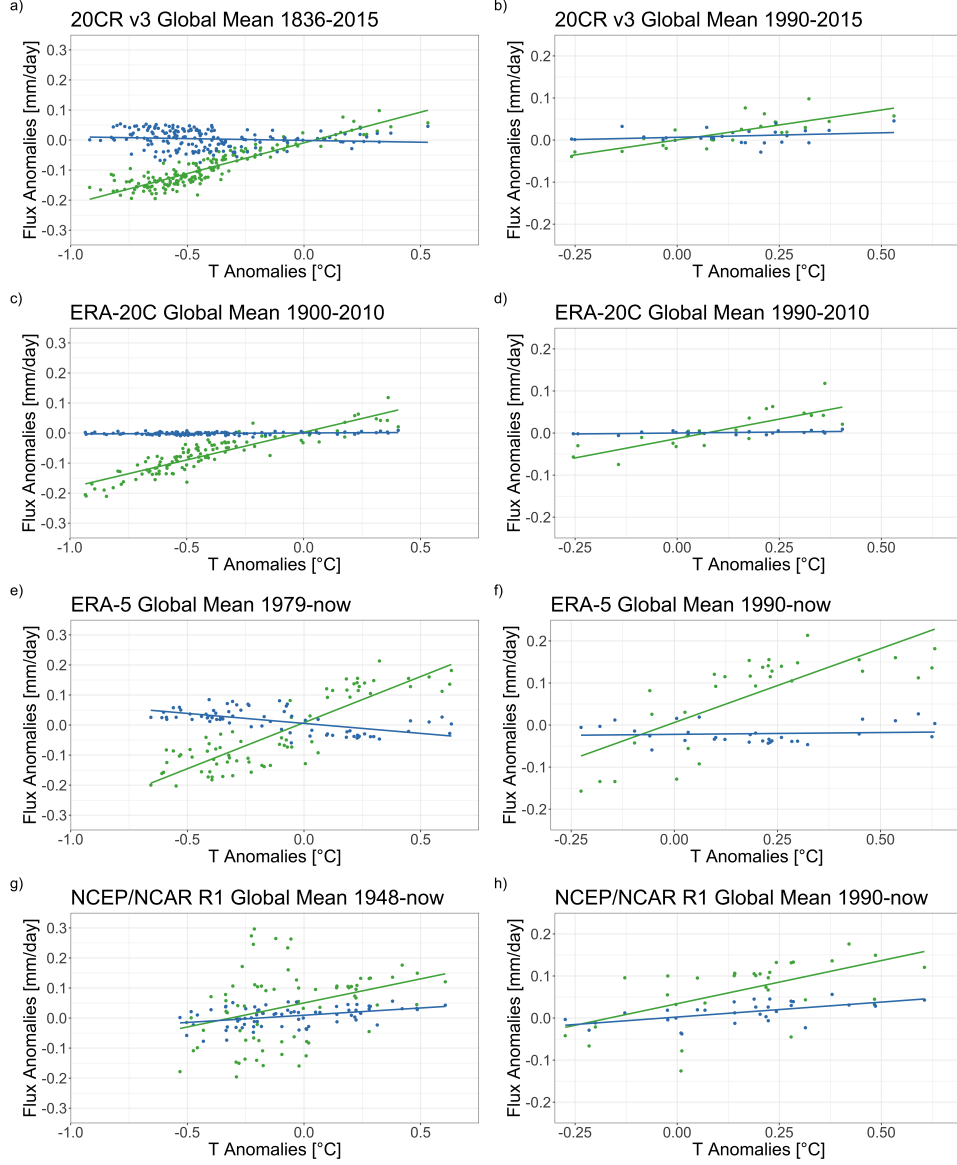5 (R = 0.094, p = 0.438); 20CR v3 (R = 0.006, p = 0.939); NCEP/NCAR R1 (R = −0.068, p = 0.569).

Because of the discrepancies observed on the time series of all four data sets around 1990, we compared the slopes for the entire record length, m, and the slopes for the 1990-onward period, m_{90} (Figure 2). The ERA-5 has the highest slope for $P+E$ and its Residual Standard Error (RSE) suggests a good linear fit ($m = 0.307$, RSE = 0.061; Figure 2.e), which increases for the 1990-now period but so does its RSE (($m_{90} = 0.352$, RSE = 0.07; Figure 2.f). When it comes to $P-E$ the slope is much smaller and negative ($m = −0.066$, RSE = 0.03; Figure 2.e), and the slope for the 1990-now is close to zero but with a lower residual standard error ($m_{90} = 0.009$, RSE = 0.023; Figure 2.f).

The 20CR v3 has a positive slope and a low residual standard error for $P+E$ ($m = 0.204$, RSE = 0.025; Figure 2.a). In the 1990-2015 period, the slope and the residual standard error decrease ($m_{90} = 0.142$, RSE = 0.021; Figure 2.b). $P-E$ has small slope and higher residual standard error for the entire record ($m = −0.012$, RSE = 0.03; Figure 2.a). However, on top of a decrease for $P-E$ residual standard error greater than observed above, for the 1990-2015 period the residual standard error is actually the lowest for the 20CR v3 ($m_{90} = 0.021$, RSE = 0.016; Figure 2.b).
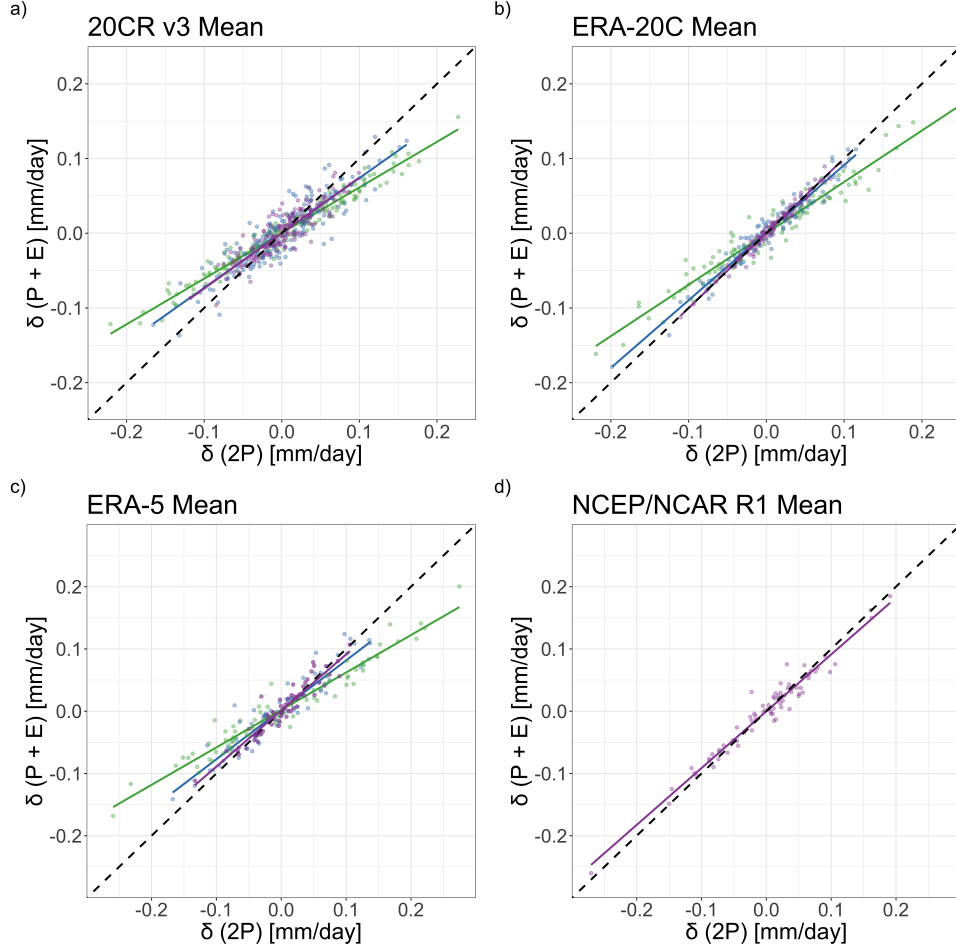
ERA-20C $P+E$ resembles that of ERA-5, because the slope for the entire record ($m = 0.184$, RSE = 0.028; Figure 2.c) increases for the 1990-2010 period ($m_{90} = 0.185$, RSE = 0.027; Figure 2.d). Notwithstanding, the residual standard error just barely decreases. Interestingly, $P-E$ has a similar behavior where the slope rises up but the residual standard error lowers down when looking at the whole record ($m = 0.003$, RSE = 0.004; Figure 2.c) and then at the 1990-2010 period ($m_{90} = 0.009$, RSE = 0.003; Figure 2.d). Note that the ERA-20C $P − E$ has the smallest residual standard errors of all the data sets regardless of the slope corresponding to the sum or the difference of precipitation and evaporation.

NCEP/NCAR R1 has the highest $P + E$ residual standard error of all data sets for its entire record ($m = 0.160$, RSE = 0.113; Figure 2.g). However, it is actually decreased by half for the 1990-now period ($m_{90} = 0.205$, RSE = 0.061; Figure 2.h). Of all the data sets, NCEP/NCAR R1 is the only whose $P − E$ slope and residual standard error reduce from the whole record ($m = 0.048$, RSE = 0.029; Figure 2.g) to the 1990-now period ($m_{90} = 0.071$, RSE = 0.021; Figure 2.h). Furthermore, while NCEP/NCAR R1 follows the general pattern of having $P + E$ slopes higher than those of $P − E$, it also has the highest $P − E$ slopes of all other data sets.

As shown in Figures 1 and 2, at the global scale and regarding the interannual and longer temporal scales, precipitation roughly equals evaporation. Given this, one could argue that $\delta(P + E) = \delta(2P)$. However, comparing these two variables reveals that across most data sets $\delta(P + E)$ is actually smaller than $\delta(2P)$ (Figure 3). Such behavior is even more evident when fractioning the data into land and ocean, wherever this is possible. We expect the global estimates to bias towards the ocean partition due to higher volumes of the atmospheric water fluxes than those over land. Still, it is interesting to see that for 20CR v3 the global and ocean curves completely overlap (Figure 3.a). ERA-20C is the only data set in which $\delta(P + E) < \delta(2P)$ for the land and ocean partitions but $\delta(P + E) = \delta(2P)$ for the global estimates (Figure 3.b). The ERA-5 has $\delta(P + E) < \delta(2P)$ for global estimates as well as for the land and ocean partitions (Figure 3.c). NCEP/NCAR R1, in agreement with ERA-5 and 20CR v3, has $\delta(P + E) < \delta(2P)$ for global estimates (Figure 3.d).

Figure 2. Average global atmospheric water fluxes anomalies in $[mm/day]$ versus temperature anomalies in $[°C]$ with respect to the 1981-2010 period, where P is precipitation, E is evaporation, and T is temperature. $P + E$ (green), $P - E$ (blue).

Figure 3. Atmospheric water flux consecutive annual variations in $[mm/day]$, where P is precipitation and E is evaporation. Global variations are in purple, land variations are in green, and ocean variations are in blue.

4 Summary and Discussion

Despite the fact that each reanalysis data set assimilates data from different sources and implements various model simulations, it is captivating to find a long-term strong positive correlation between $P+E$ and temperature at the global scale in most of the reanalysis data sets. Besides, once we estimate the annual differences, it is even more evident that the relationship between atmospheric water fluxes and the temperature is better captured by $P+E$. These overall results suggest that $P+E$ shows promise to overcome the scale limitations that hinder $P-E$ from advancing global water research further. The implementation of the $P+E$ metric as a complementary alternative, thus, could improve the detection of the intensification signal that has been inconclusive on global water cycle research while relying on the $P-E$ metric (Vargas Godoy et al., 2021).

We reported a prominent long-term superimposition of the of the annual mean global temperature and the annual mean global $P+E$ (Figure 1). Out of the four data sets analyzed herein, NCEP/NCAR R1 did not show a strong long-term correlation between $P+E$ and temperature. A possible explanation for this abnormal behavior, can be found in the apparent decoupling of the $P+E$ and temperature correlation prior the late 1970s. NCEP/NCAR R1 assimilates remote sensing data, and inconsistencies in its atmospheric data pre-1979 have already been reported and associated with the lack of satellite observations before 1979 (e.g., in the Southern Hemisphere; Tennant (2004)). Another point of interest arising from Figure 1 is the sudden decoupling of $P+E$ and temperature visible on the 20CR v3 and ERA-20C data sets after 1990, which coincides with the emergence of a strong global warming signal after 1990 (Le Mouël et al., 2005).

As discussed above, we have shown that the relationship between atmospheric water fluxes and temperature is better captured by the $P+E$ metric (Figure 1). In order to quantify this relationship and, in particular, the rate at which atmospheric water fluxes respond to changes in temperature, we looked into their slopes (Figure 2). Once again, we present that more information is gained from $P+E$ than from $P-E$ because the latter slopes are either negative or close to zero. I.e., it would be more comprehensive to describe any changes in atmospheric water fluxes as a response to an increasing temperature employing $P+E$. We inspected data from 1990 onward to look deeper into the apparent decoupling observed around that year in Figure 1. We can see that, in general, the $P+E$ slope values increase for the years after 1990. This increase suggests that the intensification signal of the global water cycle due to global warming has further strengthened in the last three decades (Greve et al., 2014).

Another point emerging from the application of $P+E$ relates to the indirect implications of Figure 3. Variations in evaporation are smaller than those of precipitation. Along such increases, a surplus of water would be transferred from the atmosphere towards the surface. Unavoidably this would lead to changes in water storage as well. Therefore, the widely used working assumption of total water storage being negligible at annual scales should be revised (Xiong et al., 2022). The second indirect implication comes when recalling that $P-E$ over land equals to $E-P$ over oceans. Inadvertently, this would mislead to a mirrored response to global warming from both partitions of the global water cycle. We know, however, that the reality is different (Roderick et al., 2014), and incorporating the $P+E$ metric it would be easier to demonstrate that land and ocean have different behaviors.

The above applications highlight the potential in using $P+E$ to measure the intensification of the water cycle at the global scale. As the socioeconomic impacts from the changes in the global water cycle are enormous, there is much space for future work. We already revealed some discrepancies between the global water cycle budget studies and the reanalysis results. It is intriguing to see how the total surface-atmosphere water transfer appears in Earth System Models and whether it can be applied as a metric for the model performance. In addition, the relationship of $P+E$ and temperature

should be investigated for purely observational estimates of global temperature to determine if the observed coupling is not an artifact of the reanalysis process. Other lines of research could explore $P+E$ spatial patterns and how they relate to regional changes and/or hydroclimatic extremes such as droughts. In this manner, quantifying the surface-atmosphere water exchange in the form of $P+E$ can enhance our insight into past, present and future hydroclimatic variability. As Dirac demonstrated in his monumental work about a century ago (Dirac, 1928), there can be enormous implications when embracing an opposite sign in the study of our natural world.

5 Open Research

The precipitation, evaporation, and temperature annual time series for all four reanalysis data sets described in Table 1 were downloaded from the KNMI Climate Explorer at `http://climexp.knmi.nl/selectfield_rea.cgi?id=someone@somewhere`

The data generated herein and the R scripts for the figures presented in the study are publicly available at `https://github.com/MiRoVaGo/P_plus_E`, and it is preserved at `https://doi.org/10.5281/zenodo.6367105`.

References

Allan, R., Barlow, M., Byrne, M. P., Cherchi, A., Douville, H., Fowler, H. J., . . . others   (2020).   Advances in understanding large-scale responses of the water cycle to climate change. *Annals of the New York Academy of Sciences*.

Dirac, P. A. M.   (1928).   The quantum theory of the electron.   *Proceedings of the Royal Society of London. Series A, Containing Papers of a Mathematical and Physical Character*, *117*(778), 610–624.

Espinoza, V., Waliser, D. E., Guan, B., Lavers, D. A., & Ralph, F. M.   (2018).   Global analysis of climate change projection effects on atmospheric rivers. *Geophysical Research Letters*, *45*(9), 4299–4308.

Fasullo, J. T.   (2010).   Robust land–ocean contrasts in energy and water cycle feedbacks. *Journal of Climate*, *23*(17), 4677–4693.

Greve, P., Orlowsky, B., Mueller, B., Sheffield, J., Reichstein, M., & Seneviratne, S. I.   (2014).   Global assessment of trends in wetting and drying over land. *Nature geoscience*, *7*(10), 716–721.

Held, I. M., & Soden, B. J.   (2006).   Robust responses of the hydrological cycle to global warming. *Journal of climate*, *19*(21), 5686–5699.

Hersbach, H., Bell, B., Berrisford, P., Hirahara, S., Horányi, A., Muñoz-Sabater, J., . . . others (2020). The era5 global reanalysis. *Quarterly Journal of the Royal Meteorological Society*, *146*(730), 1999–2049.

Huntington, T. G., Weiskel, P. K., Wolock, D. M., & McCabe, G. J. (2018). A new indicator framework for quantifying the intensity of the terrestrial water cycle. *Journal of Hydrology*, *559*, 361–372.

Kalnay, E., Kanamitsu, M., Kistler, R., Collins, W., Deaven, D., Gandin, L., . . . others   (1996).   The ncep/ncar 40-year reanalysis project.   *Bulletin of the American meteorological Society*, *77*(3), 437–472.

Le Mouël, J.-L., Kossobokov, V., & Courtillot, V. (2005). On long-term variations of

simple geomagnetic indices and slow changes in magnetospheric currents: The emergence of anthropogenic global warming after 1990? *Earth and Planetary Science Letters*, *232*(3-4), 273–286.

Oki, T., & Kanae, S. (2006). Global hydrological cycles and world water resources. *science*, *313*(5790), 1068–1072.

Pendergrass, A. G., & Hartmann, D. L. (2014). The atmospheric energy constraint on global-mean precipitation change. *Journal of climate*, *27*(2), 757–768.

Poli, P., Hersbach, H., Dee, D. P., Berrisford, P., Simmons, A. J., Vitart, F., . . . others (2016). Era-20c: An atmospheric reanalysis of the twentieth century. *Journal of Climate*, *29*(11), 4083–4097.

Roderick, M., Sun, F., Lim, W. H., & Farquhar, G. (2014). A general framework for understanding the response of the water cycle to global warming over land and ocean. *Hydrology and Earth System Sciences*, *18*(5), 1575–1589.

Slivinski, L. C., Compo, G. P., Whitaker, J. S., Sardeshmukh, P. D., Giese, B. S., McColl, C., . . . others (2019). Towards a more reliable historical reanalysis: Improvements for version 3 of the twentieth century reanalysis system. *Quarterly Journal of the Royal Meteorological Society*, *145*(724), 2876–2908.

Tennant, W. (2004). Considerations when using pre-1979 ncep/ncar reanalyses in the southern hemisphere. *Geophysical Research Letters*, *31*(11).

Vargas Godoy, M. R., Markonis, Y., Hanel, M., Kyselỳ, J., & Papalexiou, S. M. (2021). The global water cycle budget: A chronological review. *Surveys in Geophysics*, *42*(5), 1075–1107.

Xiong, J., Guo, S., Chen, J., & Yin, J. (2022). A reexamination of the dry gets drier and wet gets wetter paradigm over global land: insight from terrestrial water storage changes. *Hydrology and Earth System Sciences Discussions*, 1–20.

Yu, L., Josey, S. A., Bingham, F. M., & Lee, T. (2020). Intensification of the global water cycle and evidence from ocean salinity: a synthesis review. *Annals of the New York Academy of Sciences*, *1472*(1), 76–94.